

physica **p** status **s** solidi **s**

www.pss-journals.com

reprint



Influence of texture on the ferromagnetic properties of nanograined ZnO films

Boris Straumal^{*1,2,3}, Andrei Mazilkin^{1,2}, Svetlana Protasova^{1,2}, Ata Myatiev³, Petr Straumal^{3,4}, Eberhard Goering², and Brigitte Baretzky⁵

¹Institute of Solid State Physics, Russian Academy of Sciences, Ac. Ossipyan str. 2, 142432 Chernogolovka, Russia

²Max-Planck-Institut für Intelligente Systeme (former MPI Metallforschung), Heisenbergstrasse 3, 70569 Stuttgart, Germany

³National University of Science and Technology “MISIS”, Leninsky prospect 4, 119991 Moscow, Russia

⁴Institut für Materialphysik, Universität Münster, Wilhelm-Klemm-Str. 10, 48149 Münster, Germany

⁵Karlsruher Institut für Technologie, Institut für Nanotechnologie, Hermann-von-Helmholtz-Platz 1, 76344 Eggenstein-Leopoldshafen, Germany

Received 20 October 2010, revised 10 January 2011, accepted 11 January 2011

Published online 27 May 2011

Keywords ferromagnetism, grain boundaries, texture, zinc oxide

* Corresponding author: e-mail straumal@mf.mpg.de, Phone: +7 916 6768673, Fax: +7 49652 48291

The pure ZnO thin films were deposited by the wet chemistry ('liquid ceramics') method from the butanoate precursors on the single-crystalline (102) sapphire substrates. The films annealed in air (550 °C, 24 h) after butanoate pyrolysis have pronounced texture, and they reveal the ferromagnetic behaviour. Argon annealed films (650 °C, 30 min) exhibit randomly oriented grains, where the ferromagnetism of these non-textured films is almost equal to that of bare substrate. In both cases the films consist of dense equiaxial nanograins with size ~ 20 nm. We observed that grain boundaries (GBs) and related vacancies are the intrinsic origin for RT ferromagnetism in polycrystals

[Straumal et al., Phys. Rev. B **79**, 205206 (2009)]. Present results demonstrate that not only the specific area of GBs in nanograined ZnO alone determines the ferromagnetic behaviour of ZnO. The GB character distribution (*i.e.* GB misorientation and orientation) is different in the textured and non-textured films. Most probably, the GBs with different character possess also different magnetic properties. The role of GBs, free surfaces and interfaces in ferromagnetic behaviour of GaN is discussed. In particular, their presence permits to increase the Mn solubility in GaN without precipitation of secondary ferromagnetic phases.

© 2011 WILEY-VCH Verlag GmbH & Co. KGaA, Weinheim

1 Introduction Dietl et al. have theoretically predicted that ZnO and GaN doped by 'magnetic' atoms like Co, Mn or Fe possess ferromagnetic (FM) behaviour with a high Curie temperature T_c above room temperature (RT) [1]. This is due to carrier-related FM interactions, where the FM ordering of the transition metal (TM) ions is induced by a magnetically polarized and doping modified ZnO host. The free carriers can also induce ferromagnetic behaviour [2]. In particular, two distinct ferromagnetic mechanisms in different conductivity regimes can exist. In the insulating regime, carriers tend to be localized, favouring the formation of bound magnetic polarons, which leads to ferromagnetism. In the metallic regime, however, most carriers are weakly localized and the free carrier-mediated exchange is dominant [2]. In order to elucidate the dependence of RT ferromagnetism on the microstructure in ZnO, we have recently analyzed

a large series of experimental publications with respect to the present specific grain boundary (GB) area *i.e.* the ratio of GB area to grain volume s_{GB} [3]. FM only appears, if s_{GB} exceeds a certain threshold value s_{th} . Based on this important finding, nano-grained pure and Mn-doped ZnO films have been prepared, which reveal reproducible RT-FM, where the magnetization is proportional to the film thickness, even for pure ZnO films [3]. Our findings strongly suggested that grain boundaries and related vacancies are the intrinsic origin for RT ferromagnetism.

It is very well known for the GBs in metals that the GB character distribution (*i.e.* GB misorientation and orientation) can drastically change the properties of polycrystals [4, 5]. The goal of this work was to compare the magnetic properties of nanograined ZnO films with the same grain size (well above the threshold value s_{th}) but with different

© 2011 WILEY-VCH Verlag GmbH & Co. KGaA, Weinheim

character distribution. Similar to Ref. [3], we also discuss the influence of GBs and interface boundaries on Mn solubility and ferromagnetic behaviour of Mn-doped GaN.

2 Experimental ZnO thin films consisting of dense equiaxial nanograins were produced by using the novel method of liquid ceramics [3, 6–8]. The zinc (II) butanoate diluted in the organic solvent with zinc concentrations between 1 and 4 kg/m³ was used as a precursor for the preparation of ZnO films. The butanoate precursor was deposited on the (102) oriented sapphire single crystals. Thermal pyrolysis at 100 °C in air (about 10 min) was followed by an annealing in an electrical furnace in pure argon (650 °C, 30 min) or in air (550 °C, 24 h). Similar method was recently proposed for zinc oleates [9]. The presence of other magnetic impurities as Fe, Co and Ni was measured by atomic absorption spectroscopy in a Perkin-Elmer spectrometer and electron-probe microanalysis (EPMA). It was below 0.001 at%. The films were transparent and sometimes with a very slight greenish furnish with thicknesses between 50 and 900 nm. The thickness was determined by means of EPMA and edge-on transmission electron microscopy (TEM).

EPMA investigations were carried out in a Tescan Vega TS5130 MM microscope equipped by the LINK energy-dispersive spectrometer produced by Oxford Instruments. TEM investigations were carried out on a Jeol JEM-4000FX microscope at an accelerating voltage of 400 kV. X-ray diffraction (XRD) data were obtained on a Siemens diffractometer (Co K α 1 radiation). Evaluation of the grain or particle size (D) from the X-ray peak broadening was performed using Scherrer equation $\beta = 0.9\lambda/D\cos\theta$ where λ is the X-ray wavelength, θ the diffraction angle and β is the full-width at half maximum of the diffraction line [10]. The magnetic properties were measured on a superconducting quantum interference device SQUID (Quantum Design MPMS-7 and MPMS-XL). The magnetic field was applied parallel to the sample plane (in plane).

3 Results and discussion Figure 1 shows the dark field TEM micrograph of the nanograined pure ZnO thin film deposited on sapphire and annealed in argon. Electron diffraction pattern (inset) shows only rings from the ZnO wurtzite structure. No texture is visible. The nanocrystalline and dense film of pure ZnO consists of equiaxial grains with a mean grain size of about 20 nm. The grain size in the ZnO films deposited on sapphire and annealed in air is also about 20 nm.

Figure 2 shows the XRD spectra for ZnO thin films deposited on the (102) oriented sapphire single crystals and annealed in air (top) and in argon (bottom). The spectrum for the film annealed in argon (bottom) contains three peaks corresponding to the 100, 002 and 101 reflections of the ZnO with hexagonal wurtzite structure. However, the intensity ratio does not match the standard sample (*i.e.* powder diffraction pattern taken from a database). The most intense Bragg peak should be 101 for a random distribution which is

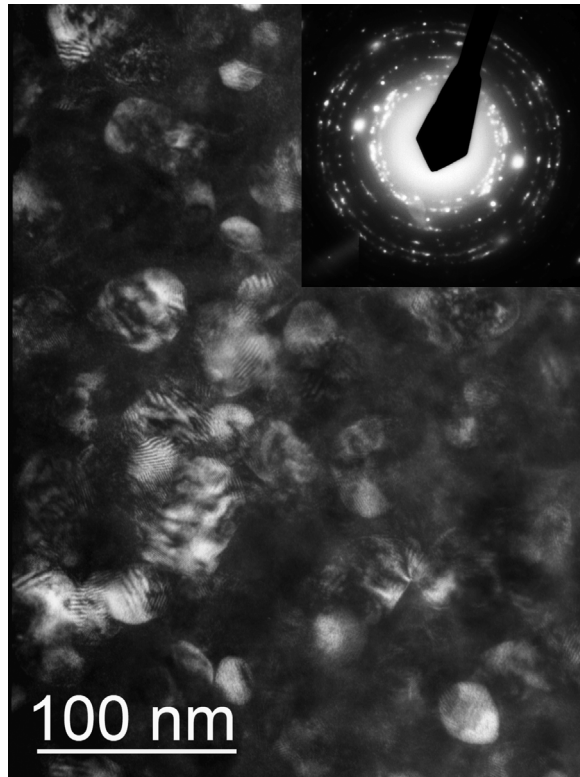


Figure 1 Dark field TEM micrograph of the nanograined pure ZnO thin film deposited on sapphire and annealed in argon. Electron diffraction pattern (inset) shows only rings from the ZnO wurtzite structure. No texture is visible.

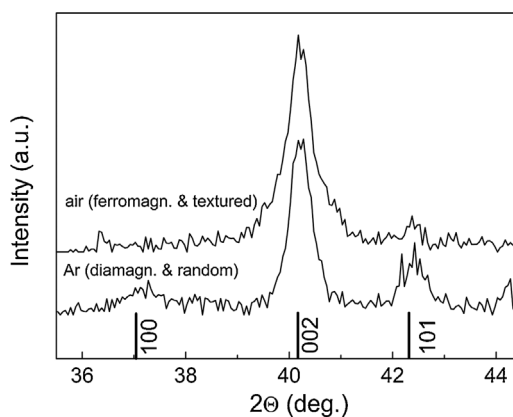


Figure 2 XRD curves for the ferromagnetic (top) and diamagnetic (bottom) ZnO thin films deposited on the (102) oriented sapphire single crystals and annealed in air (top) and in argon (bottom).

not the case. It means that the orientation of the nanograins in the ZnO film synthesized in argon is not completely random. The electron diffraction pattern for this film (see inset in the Fig. 1) contains all rings for the hexagonal wurtzite structure, but the bright spots for individual grains are not fully homogeneous distributed along each of the rings. The XRD

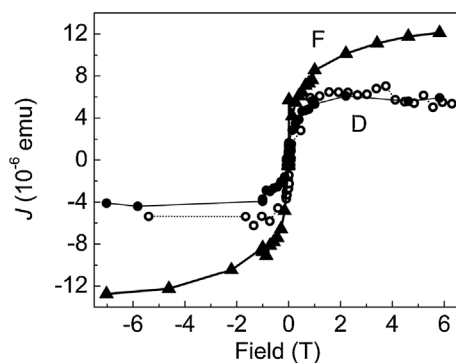


Figure 3 Magnetization (calibrated in emu) at RT for ferromagnetic (F) and diamagnetic (D) ZnO thin films annealed in air (full triangles) and in argon (full circles). Open circles show the magnetization curve for the bare sapphire substrate.

pattern and the electron diffraction pattern show different aspects of nanograin distribution in space. It is due the fact that the electron diffraction pattern is made for the very local area (few hundreds of nm) and the X-ray beams are few millimetre in diameter and permits to collect information from all grains in the sample.

The spectrum for the film annealed in air (top) contains practically the only one peak corresponding to the 002 reflections of the ZnO with hexagonal wurtzite structure. It means that the film synthesized in argon is much strongly textured than that synthesized in air. Another point which can be also mentioned here is that the width of the 002 peak for the film annealed in air is about 20% higher than that for the film annealed in argon, *i.e.* the grain size in the film annealed in air is somewhat smaller in comparison with its counterpart.

Figure 3 contains the magnetization curves for ZnO thin films annealed in air (full triangles) and in argon (full circles). The full triangles show the magnetization curve after subtraction of the input of the bare sapphire substrate. The film annealed in air clearly shows the pronounced FM indicated by the saturation of magnetization (above the applied field ~ 6 T). The film annealed in argon does not reveal the FM behaviour and remains diamagnetic. In Fig. 3 the full circles demonstrate the magnetization of ZnO thin film annealed in air after subtraction substrate diamagnetism. Open circles show the magnetization curve for the bare sapphire substrate without diamagnetism. The comparison of the latter curves shows that the ZnO film annealed in argon does not show any additional ferromagnetism with respect to the bare substrate.

The comparison of Figs. 2 and 3 demonstrates that the strongly textured ZnO film possesses the ferromagnetic behaviour and the non-textured (or weakly textured) film remains diamagnetic. We recently observed that grain boundaries and related vacancies are the intrinsic origin for RT ferromagnetism in polycrystals [3]. In Ref. [11] we concluded that the topology of the GB network in a polycrystal can also influence the magnetization of

ferromagnetic ZnO films. The GBs in ferromagnetic nanograined ZnO contain the amorphous rather irregular layers [12]. These layers in the Mn-doped ZnO concentrate the ‘magnetic’ impurity Mn [13].

Present results demonstrate that not only the specific area of GBs in nanograined ZnO alone determines the ferromagnetic behaviour of ZnO. We observed here that even when the grain size is well below the critical value for the presence of ferromagnetism for pure ZnO [3], the ferromagnetic behaviour depends on the fact whether the film is textured or not. Similar examples can be found in the literature, namely the nanograined films with specific GB area s_{GB} exceeds a certain threshold value s_{th} remain paramagnetic [13, 17, 20]. It is especially typical for the nanograined ZnO films deposited on the single crystalline sapphire substrates [13, 17, 20]. The same method like pulsed laser deposition [13, 15, 16, 20] or magnetron sputtering [14, 17, 18, 19] allows to manufacture the films with similar grain size but drastically different magnetic properties [13–20]. The GB character distribution (*i.e.* GB misorientation and orientation) is different in the textured and non-textured films. It is known the GB character distribution can drastically change the properties of polycrystals [4, 5]. Most probably, the GBs with different character in ZnO possess also different magnetic properties.

Dietl et al. predicted in their seminal work on diluted magnetic semiconductors (DMS) that the highest possible Curie temperature could be reached by Mn doping in ZnO and GaN [1]. The magnetization of ZnO depends on Mn concentration very non-monotonously [11]. In the case of GaN, the increase of Mn concentration allows to increase both magnetization and Curie temperature [21–67]. As in ZnO, the Mn concentration in GaN increases up to a certain limit. The addition of Mn above this limit leads to the formation of secondary (ferromagnetic) bulk phases deteriorating the properties of DMS. We observed recently that in case of ZnO the solubility of Mn and Co could be drastically increased without formation of secondary phases by decreasing the grain size of ZnO [6, 7]. XRD measurements demonstrated that the maximal solubility of Mn or Co in the bulk cannot be exceeded, however, the additional atoms of Mn or Co can be absorbed by intergranular, interfacial or superficial layers without formation of second phases in the bulk [6, 8, 12]. For example the solubility of Mn in ZnO at 550 °C increases from 12 at% to 33 at% in the films with 20 nm grain size [6]. Is it possible in GaN?

Indeed, the analysis of published experimental data (Fig. 4) shows that the total Mn solubility in GaN also increases with decreasing grain size. The Mn solubility is about 0.2 at% in the perfect bulk GaN single crystals containing only few dislocations [21] and becomes above 18 at% in the thin films obtained by the magnetron sputtering (grain size $d = 15$ – 18 nm [60]) and ion-assisted deposition (grain size $d = 5$ nm [61, 62]). For ZnO we found that the grain boundaries possess the higher absorbance ability in comparison with free surfaces [6, 8]. In GaN it looks that the free surfaces and interfaces with the substrate play the role

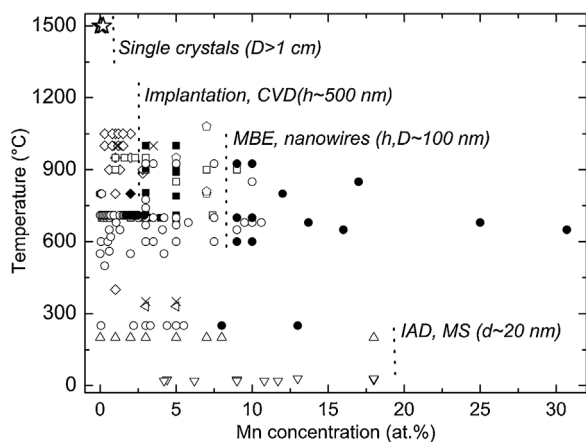


Figure 4 The presence (full symbols) or absence (open symbols) of secondary phase(s) in the Mn-doped GaN samples synthesized by various methods: bulk single crystals grown by the high-pressure method (stars [21]); films produced by the chemical vapour deposition (CVD, diamonds [22–29]) and CVD with following implantation of Mn ions (squares, [30–38]); nanowires (pentagons [39–42]); films produced by the molecular beam epitaxy (MBE, circles [43–60]), magnetron sputtering (MS, up-triangles [61]) and ion-assisted deposition (IAD, down-triangles [62, 63]); micropowders (hexagons [64]); nanopowders (left-triangles [65–67]). Vertical dotted lines mark the maximum Mn solubility for single crystals with diameter $D > 1$ cm (below 2 at%), for the films obtained by CVD or CVD with following implantation of Mn ions (film thickness $h \sim 500$ nm), for the nanowires and films deposited by MBE (h or $D \sim 100$ nm), and for the films manufactured by IAD or MS (columnar grain size $d \sim 100$ nm).

which is comparable with that of GBs. For example, the Mn solubility in the films obtained by CVD reaches at least 2.8 at% [22–29]. The Mn ion implantation into pure GaN CVD-deposited films permits to observe the formation of second phase between 2.9 and 3.1 at% Mn [30–38]. The nominally single-crystalline films obtained by CVD have almost no GBs. However, their thickness is maximally 500 nm which is at least three orders of magnitude less than in case of bulk single crystals [21]. The Mn adsorption on the free surface of CVD-films and their interface with substrate could be responsible for the Mn solubility increase from 0.2 to 3.1 at%. Also the solubility in GaN nanowires having diameter about 100 nm and no GBs the Mn solubility exceeds 7 at% [39–42]. The films produced by MBE are also nominally single-crystalline [43–60]. However, the secondary phases appear in the MBE films at 6 to 7 at% Mn. In some cases the solubility of 10–11 at% Mn is reached (Fig. 4) [44, 54]. The careful examination of published data allows to observe that the epitaxial (Ga,Mn)N films could contain the twin GBs or dislocation arrays building low-angle GBs. It is due to the fact that the (Ga,Mn)N epitaxy to the substrates like (0001) sapphire is not ideal, and the differently oriented domains with (rather perfect) twin GBs are formed in the MBE films. In our opinion, those defects together with free surface and interface with the substrate (MBE films are typically only 100–200 nm thick) could be responsible for

the increase of Mn solubility from 0.2% in the bulk single crystals [21] to 10 at% in MBE films [43–60]. Four vertical dotted lines in Fig. 4 mark the trend of the Mn solubility increase in GaN with decreasing size of GaN grains or crystals.

4 Conclusions The structure and magnetic behaviour of pure ZnO thin films deposited by the wet chemistry ('liquid ceramics') method from the butanoate precursors on the single-crystalline sapphire substrates depend on the regimes of pyrolysis and following annealing. The films annealed in air (550 °C, 24 h) have pronounced texture, and they reveal the ferromagnetic behaviour. Argon annealed films (650 °C, 30 min) have no (or very weak) texture. They remain diamagnetic. Both films have extremely fine (grain size ~ 20 nm) grain structure. Present results demonstrate that not only the specific area of GBs in nanograined ZnO alone determines the ferromagnetic behaviour of ZnO. The GB character distribution (*i.e.* GB misorientation and orientation) is different in the textured and non-textured films. Most probably, the GBs with different character possess also different magnetic properties. The role of GBs in GaN is discussed. In particular, the presence of surfaces and interfaces permits to increase the Mn solubility in GaN without precipitation of secondary ferromagnetic phases.

Acknowledgements Authors thank the Russian Foundation for Basic Research (grants 10-02-00086 and 10-02-08494), Deutsche akademische Austauschdienst (DAAD) and the Programme of Creation and Development of the National University of Science and Technology 'MISiS' for the financial support of investigations and exchange travel.

References

- [1] T. Dietl, H. Ohno, F. Matsukura, J. Cibert, and D. Ferrand, *Science* **287**, 1019 (2000).
- [2] Z. L. Lu, H. S. Hsu, Y. H. Tzeng, F. M. Zhang, Y. W. Du, and J. C. A. Huang, *Appl. Phys. Lett.* **95**, 102501 (2009).
- [3] B. B. Straumal, A. A. Mazilkin, S. G. Protasova, A. A. Myatiev, P. B. Straumal, G. Schütz, P. A. van Aken, E. Goering, and B. Baretzky, *Phys. Rev. B* **79**, 205206 (2009).
- [4] S. Kobayashi, S. Tsurekawa, T. Watanabe, and G. Palumbo, *Scr. Mater.* **62**, 294 (2010).
- [5] S. Tsurekawa, K. Okamoto, K. Kawahara, and T. Watanabe, *J. Mater. Sci.* **40**, 895 (2005).
- [6] B. B. Straumal, B. Baretzky, A. A. Mazilkin, S. G. Protasova, A. A. Myatiev, and P. B. Straumal, *J. Eur. Ceram. Soc.* **29**, 1963 (2009).
- [7] B. B. Straumal, A. A. Mazilkin, P. B. Straumal, and A. A. Myatiev, *Int. J. Nanomanufact.* **2**, 253 (2008).
- [8] B. B. Straumal, A. A. Mazilkin, S. G. Protasova, A. A. Myatiev, P. B. Straumal, and B. Baretzky, *Acta Mater.* **56**, 6246 (2008).
- [9] W. S. Chiu, P. S. Khiew, D. Isa, M. Cloke, S. Radiman, R. Abd-Shukor, M. H. Abdullah, and N. M. Huang, *Chem. Eng. J.* **142**, 337 (2008).
- [10] L. Lábár, *Microsc. Microanal.* **14**, 287 (2008).

- [11] B. B. Straumal, S. G. Protasova, A. A. Mazilkin, A. A. Myatiev, P. B. Straumal, G. Schütz, E. Goering, and B. Baretzky, *J. Appl. Phys.* **108**, 073923 (2010).
- [12] B. B. Straumal, A. A. Myatiev, P. B. Straumal, A. A. Mazilkin, S. G. Protasova, E. Goering, and B. Baretzky, *JETP Lett.* **92**, 433 (2010).
- [13] J. W. Lee, S. Kuroda, F. Takano, H. Akinaga, and K. Takita, *Phys. Status Solidi C* **3**, 4098 (2006).
- [14] F.-Y. Ran, M. Imaoka, M. Tanemura, Y. Hayashi, T.-S. Heng, and S.-P. Lau, *Phys. Status Solidi B* **246**, 1243 (2009).
- [15] Q. Xu, H. Schmidt, S. Zhou, K. Potzger, M. Helm, H. Hochmuth, M. Lorenz, A. Setzer, P. Esquinazi, Chr. Meinelcke, and M. Grundmann, *Appl. Phys. Lett.* **92**, 082508 (2008).
- [16] M. Diaconu, H. Schmidt, H. Hochmuth, M. Lorenz, G. Benndorf, J. Lenzner, D. Spemann, A. Setzer, K.-W. Nielsen, P. Esquinazi, and M. Grundmann, *Thin Solid Films* **486**, 117 (2005).
- [17] G.-H. Ji, Z.-B. Gu, M.-H. Lu, D. Wu, S.-T. Zhang, Y.-Y. Zhu, S.-N. Zhu, and Y.-F. Chen, *J. Phys.: Condens. Matter* **20**, 425207 (2008).
- [18] J. Elanchezhian, K. P. Bhuvana, N. Gopalakrishnan, and T. Balasubramanian, *Mater. Lett.* **62**, 3379 (2008).
- [19] D. F. Wang, S. Y. Park, H. W. Lee, Y. S. Lee, V. D. Lam, and Y. P. Lee, *Phys. Status Solidi A* **204**, 4029 (2007).
- [20] H. Schmidt, M. Diaconu, H. Hochmuth, M. Lorenz, A. Setzer, P. Esquinazi, A. Pöpl, D. Spemann, K.-W. Nielsen, R. Gross, G. Wagner, and M. Grundmann, *Superlattices Microstruct.* **39**, 334 (2006).
- [21] A. Wolos, A. Wyszomolek, M. Kaminska, A. Twardowski, M. Bockowski, I. Grzegory, S. Porowski, and M. Potemski, *Phys. Rev. B* **70**, 245202 (2004).
- [22] Z. G. Hu, A. B. Weerasekera, N. Dietz, A. G. U. Perera, M. Strassburg, M. H. Kane, A. Asghar, and I. T. Ferguson, *Phys. Rev. B* **75**, 205320 (2007).
- [23] M. H. Kane, S. Gupta, W. E. Fenwick, N. Li, E.-H. Park, M. Strassburg, and I. T. Ferguson, *Phys. Status Solidi A* **204**, 61 (2007).
- [24] M. H. Kane, M. Strassburg, W. E. Fenwick, A. Asghar, J. Senawiratne, D. Azamat, Z. Hu, E. Malguth, S. Graham, U. Perera, W. Gehlhoff, A. Hoffmann, N. Dietz, C. J. Summers, and I. T. Ferguson, *Phys. Status Solidi C* **3**, 2237 (2006).
- [25] M. L. Reed, M. J. Reed, M. O. Luen, E. A. Berkman, F. E. Arkun, S. M. Bedair, J. M. Zavada, and N. A. El-Masry, *Phys. Status Solidi C* **2**, 2403 (2005).
- [26] M. L. Reed, N. A. El-Masry, H. H. Stadelmaier, M. K. Ritums, M. J. Reed, C. A. Parker, J. C. Roberts, and S. M. Bedair, *Appl. Phys. Lett.* **79**, 3473 (2001).
- [27] I. T. Ferguson, *Phys. Status Solidi C* **4**, 389 (2007).
- [28] C. H. Choi, S. H. Kim, and M. H. Jung, *J. Magn. Magn. Mater.* **321**, 3833 (2009).
- [29] X. L. Yang, W. X. Zhu, C. D. Wang, H. Fang, T. J. Yu, I. Z. J. Yang, G. Y. Zhang, X. B. Qin, R. S. Yu, and B. Y. Wang, *Appl. Phys. Lett.* **94**, 151907 (2009).
- [30] Y. Shon, Y. H. Kwon, Sh. U. Yuldashev, J. H. Leem, C. S. Park, D. J. Fu, H. J. Kim, and T. W. Kang, *Appl. Phys. Lett.* **81**, 1845 (2002).
- [31] N. Theodoropoulou, A. F. Hebard, M. E. Overberg, C. R. Abernathy, S. J. Pearton, S. N. G. Chu, and R. G. Wilson, *Appl. Phys. Lett.* **78**, 3475 (2001).
- [32] Y. Shi, Y.-X. Zhang, C.-Z. Jiang, D.-J. Fu, and X.-J. Fan, *Physica B* **388**, 82 (2007).
- [33] L. L. Guo, W. Z. Shen, and Y. H. Zhang, *J. Appl. Phys.* **99**, 113533 (2006).
- [34] V. A. Chitta, J. A. H. Coaquira, J. R. L. Fernandez, C. A. Duarte, J. R. Leite, D. Schikora, D. J. As, K. Lischka, and E. Abramof, *Appl. Phys. Lett.* **85**, 3777 (2004).
- [35] J. M. Baik, H. S. Kim, C. G. Park, and J.-L. Lee, *Appl. Phys. Lett.* **83**, 2632 (2003).
- [36] N. Theodoropoulou, M. E. Overberg, S. N. G. Chu, A. F. Hebard, C. R. Abernathy, R. G. Wilson, J. M. Zavada, K. P. Lee, and S. J. Pearton, *Phys. Status Solidi B* **228**, 337 (2001).
- [37] D. Xu, Y. Zhang, Y. Zhang, P. Li, and C. Wang, *J. Magn. Magn. Mater.* **321**, 2242 (2009).
- [38] L. Sun, F. Yan, H. Gao, H. Zhang, Y. Zeng, G. Wang, and J. Li, *J. Phys. D, Appl. Phys.* **41**, 165004 (2008).
- [39] E. Oha, J. H. Choi, H.-K. Seong, and H.-J. Choi, *Appl. Phys. Lett.* **89**, 092109 (2006).
- [40] C. Xu, J. Chun, K. Rho, D. E. Kim, B. J. Kim, S. Yoon, S.-E. Han, and J.-J. Kim, *J. Appl. Phys.* **99**, 064312 (2006).
- [41] S.-E. Han, H. Oh, J.-J. Kim, H.-K. Seong, and H.-J. Choi, *Appl. Phys. Lett.* **87**, 062102 (2005).
- [42] D. S. Han, J. Park, K. W. Rhie, S. Kim, and J. Chang, *Appl. Phys. Lett.* **86**, 032506 (2005).
- [43] S. Wei, W. Yan, Z. Sun, Q. Liu, W. Zhong, X. Zhang, H. Oyanagi, and Z. Wu, *Appl. Phys. Lett.* **89**, 121901 (2006).
- [44] O. Sancho-Juan, A. Cantarero, G. Martínez-Criado, D. Oluín, N. Garro, A. Cros, M. Salomé, J. Susini, S. Dhar, and K. Ploog, *Phys. Status Solidi B* **243**, 1692 (2006).
- [45] J. I. Hwang, Y. Ishida, M. Kobayashi, Y. Osafune, T. Mizokawa, A. Fujimori, Y. Takeda, K. Terai, S.-I. Fujimori, Y. Saitoh, Y. Muramatsu, A. Tanaka, T. Kondo, H. Mune-kata, M. Hashimoto, H. Tanaka, S. Hasegawa, and H. Asahi, *Phys. Status Solidi B* **243**, 1696 (2006).
- [46] B. He, X. Zhang, S. Wei, H. Oyanagi, S. V. Novikov, K. W. Edmonds, C. T. Foxon, G. Zhou, and Y. Jia, *Appl. Phys. Lett.* **88**, 051905 (2006).
- [47] F. Takano, H. Ofuchi, J. W. Leec, K. Takita, and H. Akinaga, *Physica B* **376**, 658 (2006).
- [48] J. I. Hwang, Y. Ishida, M. Kobayashi, H. Hirata, K. Takubo, T. Mizokawa, A. Fujimori, J. Okamoto, K. Mamiya, Y. Saito, Y. Muramatsu, H. Ott, A. Tanaka, T. Kondo, and H. Mune-kata, *Phys. Rev. B* **72**, 085216 (2005).
- [49] H. C. Jeon, T. W. Kang, T. W. Kim, Kang. Joongoo, and K. J. Chang, *Appl. Phys. Lett.* **87**, 092501 (2005).
- [50] J. Chang, G. Kimb, W.-Y. Lee, and J.-M. Myoung, *Thin Solid Films* **472**, 144 (2005).
- [51] I. T. Yoon, T. W. Kang, M. C. Jeong, M. H. Ham, and J. M. Myoung, *Appl. Phys. Lett.* **85**, 4878 (2004).
- [52] K. J. Lee, K. H. Kim, F. C. Yu, W. S. Im, C. X. Gao, D. J. Kim, H. J. Kim, and Y. E. Ihm, *Phys. Status Solidi B* **241**, 2854 (2004).
- [53] K. H. Kim, K. J. Lee, H. S. Kang, F. C. Yu, J. A. Kim, D. J. Kim, K. H. Baik, S. H. Yoo, C. G. Kim, Y. S. Kim, C. S. Kim, H. J. Kim, and Y. E. Ihm, *Phys. Status Solidi B* **241**, 1458 (2004).
- [54] H. Nakayama, H. Mashita, E. Kulatov, R. Funahash, and H. Ohta, *J. Magn. Magn. Mater.* **258**, 323 (2003).
- [55] H. Hori, S. Sonoda, T. Sasaki, Y. Yamamoto, S. Shimizu, K. Suga, and K. Kindo, *Physica B* **324**, 142 (2002).
- [56] G. Thaler, R. Frazier, B. Gila, J. Stapleton, M. Davidson, C. R. Abernathy, S. J. Pearton, and Segre. Carlos, *Appl. Phys. Lett.* **84**, 2578 (2004).

- [57] D. Mai, T. Niermann, J. Zenneck, M. Roever, A. Bedoya Pinto, J. Malindretos, M. Seibt, and A. Rizzi, *Phys. Status Solidi C* **5**, 1832 (2008).
- [58] K. H. Lee, J. Y. Lee, J. H. Jung, T. W. Kim, H. C. Jeon, and T. W. Kang, *Appl. Phys. Lett.* **92**, 141919 (2008).
- [59] G. Martínez-Criado, A. Somogyi, A. Homs, R. Tucoulou, and J. Susini, *Appl. Phys. Lett.* **87**, 061913 (2005).
- [60] S. Kuroda, E. Bellet-Amalric, R. Giraud, S. Marcet, J. Cibert, and H. Mariette, *Appl. Phys. Lett.* **82**, 4580 (2003).
- [61] D. M. G. Leite, L. F. da Silva, A. L. J. Pereira, and J. H. Diasda Silva, *J. Cryst. Growth* **294**, 309 (2006).
- [62] S. Granville, B. J. Ruck, F. Budde, H. J. Trodahl, and G. V. M. Williams, *Phys. Rev. B* **81**, 184425 (2010).
- [63] S. Granville, B. J. Ruck, A. R. H. Preston, T. Stewart, F. Budde, H. J. Trodahl, A. Bittar, J. E. Downes, and M. Ridgway, *J. Appl. Phys.* **104**, 103710 (2008).
- [64] H. Li, B. Song, H. Q. Bao, G. Wang, W. J. Wang, and X. L. Chen, *J. Magn. Magn. Mater.* **321**, 222 (2009).
- [65] S. Granville, F. Budde, B. J. Ruck, H. J. Trodahl, G. V. M. Williams, A. Bittar, M. Ryan, J. Kennedy, A. Markwitz, J. B. Metson, K. E. Prince, J. M. Cairney, and M. C. Ridgway, *J. Appl. Phys.* **100**, 084310 (2006).
- [66] K. Biswas, K. Sardar, and C. N. R. Rao, *Appl. Phys. Lett.* **89**, 132503 (2006).
- [67] J. B. Gosk, M. Drygas, J. F. Janik, M. Palczewska, R. T. Paine, and A. Twardowski, *J. Phys. D, Appl. Phys.* **39**, 3717 (2006).